

doi <http://dx.doi.org/10.18265/2447-9187a2022id7759>

ORIGINAL ARTICLE

SUBMITTED June 1, 2022

APPROVED September 11, 2023

PUBLISHED ONLINE October 18, 2023


FINAL FORMATTED VERSION December 2, 2024

ASSOCIATE EDITOR  
Manoel Barbosa Dantas

# Evaluation of surfactant nonylphenol polyethoxylated 9.5 as a corrosion inhibitor of SAE1020 steel in saline medium


 Gecílio Pereira da Silva <sup>[1]</sup> \*

 Luiz Ferreira da Silva Filho <sup>[2]</sup>

 Alessandro Alisson de Lemos Araujo <sup>[3]</sup>

 Victor Augusto Freire Costa <sup>[4]</sup>

 Richelly Nayhene de Lima <sup>[5]</sup>

 Simone Cristina Freitas Carvalho <sup>[6]</sup>

[1] [gecilio@ufersa.edu.br](mailto:gecilio@ufersa.edu.br)

[2] [luiz.filho@ufersa.edu.br](mailto:luiz.filho@ufersa.edu.br)

[3] [alessandro.lemos@ufersa.edu.br](mailto:alessandro.lemos@ufersa.edu.br)

[4] [victoragusto\\_costa@hotmail.com](mailto:victoragusto_costa@hotmail.com)

[6] [simone.carvalho@ufersa.edu.br](mailto:simone.carvalho@ufersa.edu.br)  
Engineering Center, Federal Rural University of the Semiarid (UFERSA), Pau dos Ferros, Rio Grande do Norte, Brazil

[5] [richellylima04@gmail.com](mailto:richellylima04@gmail.com)  
Center of Exact and Natural Sciences, Federal Rural University of the Semiarid (UFERSA), Mossoró, Rio Grande do Norte, Brazil

\* Corresponding author.

**ABSTRACT:** Due to its relatively low cost and good chemical stability, nonylphenol polyethoxylated with an ethoxylation degree of 9.5 (NPE95) is produced on a large scale and widely used in the industry as an emulsifier, detergent, and solubilizer. Despite its extensive applicability, there is a gap in the literature regarding its corrosion inhibition properties. This study evaluated the surfactant NPE95 as a corrosion inhibitor for SAE1020 steel in 3% NaCl aqueous solution at concentrations of 5 ppm, 10 ppm, and 25 ppm. Measurements of mass loss and visual and microscopic verification of the corrosion products on the metal surface were performed using photographic records obtained with an Olympus® SZ61 optical stereoscope and an Olympus® BX51M microscope. In addition to these techniques, electrochemical impedance spectroscopy (EIS) was conducted using an AUTOLAB PGSTAT 204 potentiostat/galvanostat to better confirm the surfactant's inhibitory potential. The impedance results with the inhibitor in the corrosive medium show two capacitive arcs. The first capacitive arc is attributed to the adsorbed film on carbon steel, while the second, at low frequencies, indicates a charge transfer process at the metal/electrolyte interface, or corrosion process. The  $\Delta G_{ads}$  values obtained from the Langmuir and El-Awady models were  $-21.987 \text{ kJ.mol}^{-1}$  and  $-10.061 \text{ kJ.mol}^{-1}$ , respectively, indicating spontaneous physisorption processes. Data on total mass loss showed that the lowest mass loss occurred in the sample exposed to the highest surfactant concentration (25 ppm), demonstrating a reduction of approximately 17% in the corrosion rate in the saline medium.

**Keywords:** adsorption; corrosion inhibitor; electrochemical impedance spectroscopy; polyethoxylated nonylphenol; surfactant.

## Avaliação do surfactante nonilfenol polietoxilado 9,5 como inibidor de corrosão do aço SAE1020 em meio salino

**RESUMO:** Devido ao seu baixo custo e boa estabilidade química, o nonilfenol polietoxilado com grau de etoxilação de 9,5 (NPE95) é produzido em larga escala



e amplamente utilizado na indústria como emulsificante, detergente e solubilizante. Apesar de sua ampla aplicabilidade, há uma lacuna na literatura sobre suas propriedades inibidoras de corrosão. Este estudo avaliou o surfactante NPE95 como inibidor de corrosão para o aço SAE1020 em solução aquosa de NaCl a 3%, nas concentrações de 5 ppm, 10 ppm e 25 ppm de inibidor. Foram realizadas medições de perda de massa e verificação visual e microscópica dos produtos de corrosão na superfície metálica por meio de registros fotográficos obtidos com um estereoscópio óptico Olympus® SZ61 e um microscópio Olympus® BX51M. Além dessas técnicas, foi realizada a espectroscopia de impedância eletroquímica (EIE) utilizando um potenciostato/galvanostato AUTOLAB PGSTAT 204 para melhor confirmar o potencial inibidor do surfactante. Os resultados de impedância com o inibidor no meio corrosivo apresentaram dois arcos capacitivos. O primeiro arco capacitivo foi atribuído ao filme adsorvido no aço carbono, enquanto o segundo, em baixas frequências, indicou um processo de transferência de carga na interface metal/eletrólito, ou processo de corrosão. Os valores de  $\Delta G_{ads}$  obtidos pelos modelos de Langmuir e El-Awady foram, respectivamente,  $-21,987 \text{ kJ.mol}^{-1}$  e  $-10,061 \text{ kJ.mol}^{-1}$ , indicando processos espontâneos de fisissorção. Os dados de perda de massa total mostraram que a menor perda de massa ocorreu na amostra exposta à maior concentração de surfactante (25 ppm), demonstrando uma redução de aproximadamente 17% na taxa de corrosão no meio salino.

**Palavras-chave:** adsorção; espectroscopia de impedância eletroquímica; inibidor de corrosão; nonilfenol polietoxilado; surfactante.

## 1 Introduction

The corrosion of metals results in significant inconveniences and material damage across various industrial activities, incurring substantial direct and indirect costs. Such occurrences can lead to downtime for maintenance and replacement of components, loss of products, reduced efficiency of production systems, and environmental contamination, among other issues. In extreme cases, sudden fractures of critical equipment parts can cause severe accidents, including loss of human lives. The pursuit of developing and improving techniques for corrosion control and mitigation is a contemporary topic that has garnered considerable attention from many researchers (Dwivedi; Lepková; Becker, 2017; Goyal *et al.*, 2018).

Carbon steel is the primary metallic material used in mechanical construction due to its properties and relatively low cost (Dwivedi; Lepková; Becker, 2017). However, its high susceptibility to corrosive processes in various environments necessitates the application of appropriate corrosion protection and control methods (Dwivedi; Lepková; Becker, 2017; El-Haddad *et al.*, 2019; Refait *et al.*, 2020). Among natural corrosive environments, seawater is one of the most aggressive to steel because salts present accelerate the corrosive process (Refait *et al.*, 2020).

The use of corrosion inhibitors to protect steels in aqueous media has proven to be a highly efficient solution to minimizing or even preventing corrosion when properly specified and applied. The most general classification of these inhibitors into cathodic, anodic, and adsorption is based on their protection mechanisms (Brycki *et al.*, 2017). Cathodic and anodic inhibitors form insoluble products that act as a barrier in the cathodic and anodic regions, respectively, while adsorption inhibitors can form protective films

over the entire areas of interest, interfering with the electrochemical reactions involved (Brycki *et al.*, 2017; Pedefferri, 2018). In the latter categories, organic molecules with strongly polar groups are prominent, particularly surfactants. These compounds are widely used in a variety of applications due to their intrinsic ability to interact with both polar and non-polar substances. They are characterized by their capability to interact with oils, fats, and interfaces of solutions containing solids, liquids, including water, and gases, often interacting simultaneously with both (Sarkar *et al.*, 2021; Shaban; Kang; Kim, 2020; Tiwari; Mall; Solanki, 2018).

The surfactant nonylphenol polyethoxylated 9.5 (NPE95) is a non-ionic surfactant whose hydrophobic part of the molecule is derived from nonylphenol, and the hydrophilic part comes from the ethylene oxide chain (Rodrigues *et al.*, 2021). Due to its relatively low cost and good chemical stability, NPE95 is produced on a large scale and widely used in the industry as an emulsifier, detergent, and solubilizer, among other applications. Despite its extensive applicability, there is a gap in the literature regarding its corrosion inhibition properties.

This study evaluates the protection efficiency of the surfactant NPE95 as a corrosion inhibitor for SAE1020 carbon steel in 3.0% NaCl medium, using methods of electrochemical impedance spectroscopy (EIS) and mass loss.

This study examines the theoretical foundations of corrosion inhibitors in Section 2. Section 3 details the experimental methods employed, including Electrochemical Impedance Spectroscopy (EIS) and the mass loss technique, to assess the effectiveness of NPE95. The results and discussion, presented in Section 4, emphasize the influence of inhibitor concentration on polarization resistance and corrosion rate. A comparison of the experimental data with adsorption isotherm models is also provided, demonstrating the behavior of NPE95 in mitigating corrosion in saline environments.

## 2 Theoretical reference

This section explores the theoretical aspects of corrosion inhibitors, with a particular focus on the mechanisms through which they operate, primarily via adsorption onto metal surfaces. Special attention is devoted to using nonylphenol polyethoxylate 9.5 (NPE95) as a corrosion inhibitor for SAE1020 steel in saline conditions. Additionally, an overview of electrochemical techniques, such as Electrochemical Impedance Spectroscopy (EIS), is presented, highlighting their application in evaluating the efficiency of corrosion inhibitors.

### 2.1 Corrosion inhibitors by adsorption

Corrosion inhibitors are chemical substances designed to slow down or prevent the corrosion of metals. Some adsorption inhibitors exhibit detergent-like properties, creating space amidst impurities on the metal surface and forming a protective film. These inhibitors function by forming a protective layer on the metal surface, thereby preventing corrosive ions from coming into contact with it. This layer forms when the inhibitor adsorbs onto the metal surface, creating a physical barrier that reduces the corrosion rate. The effectiveness of adsorption corrosion inhibitors depends on factors such as the nature of the inhibitor, its concentration, temperature, and the agitation of the corrosive medium (Brycki *et al.*, 2017).

The theoretical fractions of adsorbed molecules or degree of coverage ( $\theta$ ) and inhibition efficiencies ( $\eta$ ) can be calculated from Equations 1 and 2 (Javadian; Yousefi; Neshati, 2013).

$$\theta = \frac{n\%}{100} \quad (1)$$

$$\eta\% = \frac{R_p - R_{p_0}}{R_p} \times 100 \quad (2)$$

where  $R_p$  is the polarization resistance of the material with the inhibitor and  $R_{p_0}$  is the polarization resistance without the inhibitor.

## 2.2 Nonylphenol polyethoxylate 9.5 (NPE95)

Nonylphenol polyethoxylate with an average number of 9.5 ethoxylate units (NPE95) is a non-ionic surfactant (molecular weight ( $W$ ) = 617 g.mol<sup>-1</sup>, complete solubility in water, viscosity 230-270 mPa.s at 25 °C, density 1,060 kg.m<sup>-3</sup>). NPE95 is a chemical compound containing a nonylphenol base with a polyethylene oxide chain that has, on average, 9.5 ethylene oxide units. This compound is commonly used in various industrial applications, including as an emulsifier, detergent, and solubilizer (Melo *et al.*, 2014).

## 2.3 Electrochemical impedance spectroscopy (EIS)

Electrochemical Impedance Spectroscopy (EIS) is a powerful technique for the real-time evaluation of the effectiveness of corrosion inhibitors. This technique involves applying a small amplitude alternating signal to an electrochemical system and subsequent analysis of the resulting frequency response. EIS allows for the characterization of the corrosion resistance of the metallic surface and the efficiency of the corrosion inhibitor. Parameters obtained from EIS measurements include polarization resistance ( $R_p$ ), electric double-layer capacitance ( $C_p$ ), and the time constant associated with the inhibitor adsorption processes. These parameters provide crucial information regarding the action of the inhibitor on the metal surface and its influence on the corrosion rate (Ribeiro; Souza; Abrantes, 2015).

Polarization resistance can be assessed from the Nyquist diagram, which consists of a scatter plot in the complex plane, where the real part of impedance (resistance) is plotted on the horizontal axis ( $Z'$ ) and the imaginary part (reactance) is plotted on the vertical axis ( $Z''$ ). After constructing the Nyquist diagram, extrapolation is performed from the right-hand side of the semicircle until it intersects the horizontal axis. The diameter of the semicircle represents the charge transfer resistance ( $R_t$ ), which is equivalent to the polarization resistance ( $R_p$ ). Thus, the larger the diameter of this semicircle, the higher the  $R_p$  resistance and, consequently, the lower the corrosion rate (CR) (Ribeiro; Souza; Abrantes, 2015).

### 3 Experimental

The inhibitory action of the NPE95 on SAE1020 steel in 3.0% NaCl medium was evaluated using electrochemical impedance spectroscopy (EIS). This analysis was conducted with an AUTOLAB PGSTAT 204 potentiostat/galvanostat, from Methron Autolab®, utilizing NOVA software version 2.0 for data acquisition and parameters analysis. Tests were performed at open circuit potential, at room temperature, with a frequency range from 10 kHz to 4 MHz, an amplitude of 0.01 V, and a potential stabilization time of 10 minutes before the start of each experiment to achieve a steady-state open circuit potential. The experiments were conducted in a conventional electrochemical cell with an 80.0 mL capacity, comprising three electrodes: an Ag(s)|AgCl(s)|Cl-(aq., [Cl-]) reference electrode; a platinum plate with an approximate geometric area of 2.0 cm<sup>2</sup> as the counter electrode; and a SAE1020 steel disk with an exposed circular surface area of approximately 1.0 cm<sup>2</sup> as the working electrode. A Faraday cage was employed to obtain the impedance diagrams.

Before testing, the working electrodes were polished with silicon carbide paper of decreasing granulation: 320, 400, 500, and 1,200 mesh. The polished electrodes were cleaned in an ultrasonic bath using bidistilled water and acetone. Experiments were conducted by adding sufficient amounts of surfactant to the corrosive medium to achieve concentrations of 5.0 ppm, 10.0 ppm, and 25.0 ppm. For comparison, analyses were also performed without the addition of the surfactant.

Polarization resistances ( $R_p$ ) obtained via EIS and the surfactant concentrations in the corrosive media were used to construct adsorption curves. Through linear regression, correlation coefficients ( $R^2$ ) were obtained and used to select the most appropriate adsorption isotherm models (Arellanes-Lozada *et al.*, 2018; Farsak; Keles; Keles, 2015). Theoretical fractions of adsorbed molecules ( $\theta$ ) and inhibition efficiencies ( $\eta$ ) were calculated using Equations 1 and 2, respectively.

The spontaneity of surfactant adsorption processes on the steel surface was calculated for each experiment, determining the free adsorption energies  $\Delta G_{ads}$  (kJ.mol<sup>-1</sup>) using Equation 3 (Javadian; Yousefi; Neshati, 2013):

$$K_{ads} = \left( \frac{1}{55.5} \right) \exp \left( \frac{\Delta G_{ads}}{RT} \right) \quad (3)$$

where  $T$  is the absolute temperature,  $R$  is the gas constant, and  $K_{ads}$  is the equilibrium adsorption constant of the evaluated isotherm models.

To confirm the EIS results, the corrosion-inhibiting action of NPE95 was evaluated using the mass loss method. These experiments were conducted in duplicate, following NACE RP0775, NACE TM169, and ASTM G1 standards (ASTM International, 1999; Bajares; Mella, 2015; NACE International, 1999). The specimens used were SAE1020 carbon steel coupons® from Roxar Flow Measurement AS®, disk-shaped with a central hole, as illustrated in Figure 1.

**Figure 1** ▶

Typical images of coupons used in mass loss corrosion tests obtained with 8× magnification.  
Source: authors' archive



**Table 1** ▼

Initial mass and dimensions of the exposed area of the coupons.  
Source: research data

The dimensions of the disks, holes, and thicknesses were measured using a digital caliper with a precision of 0.01 mm, Mitutoyo® Absolute Digimatic model. Weighings were performed on an Ohaus® Adventurer model analytical balance with an accuracy of four decimal places. Images of the longitudinal and transversal sections were obtained using an Olympus® SZ61 optical stereoscope, with an 8× magnification. The initial masses and dimensions of the coupons are shown in Table 1.

Description	Mass (g)	Dimensions (mm)	Height (mm)	Exposed area (mm <sup>2</sup> )
Absence of surfactant	20.5726	$\Phi = 32.13$ $\Phi_{IM} = 17.50$ $\Phi_{im} = 9.95$	4.05	1,950.81
Solution with 5 ppm (1)	20.8614	$\Phi = 32.10$ $\Phi_{IM} = 17.57$ $\Phi_{im} = 9.99$	4.13	1,956.886
Solution with 5 ppm (2)	20.6960	$\Phi = 32.10$ $\Phi_{IM} = 17.52$ $\Phi_{im} = 10.03$	4.10	1,952.249
Solution with 10 ppm (1)	20.7865	$\Phi = 32.11$ $\Phi_{IM} = 17.48$ $\Phi_{im} = 9.99$	4.09	1,953.090
Solution with 10 ppm (2)	20.7532	$\Phi = 32.09$ $\Phi_{IM} = 17.10$ $\Phi_{im} = 10.01$	4.09	1,952.021
Solution with 25 ppm (1)	20.4470	$\Phi = 32.06$ $\Phi_{IM} = 17.51$ $\Phi_{im} = 9.97$	4.06	1,943.742
Solution with 25 ppm (2)	20.6760	$\Phi = 32.12$ $\Phi_{IM} = 17.13$ $\Phi_{im} = 9.95$	4.02	1,947.276

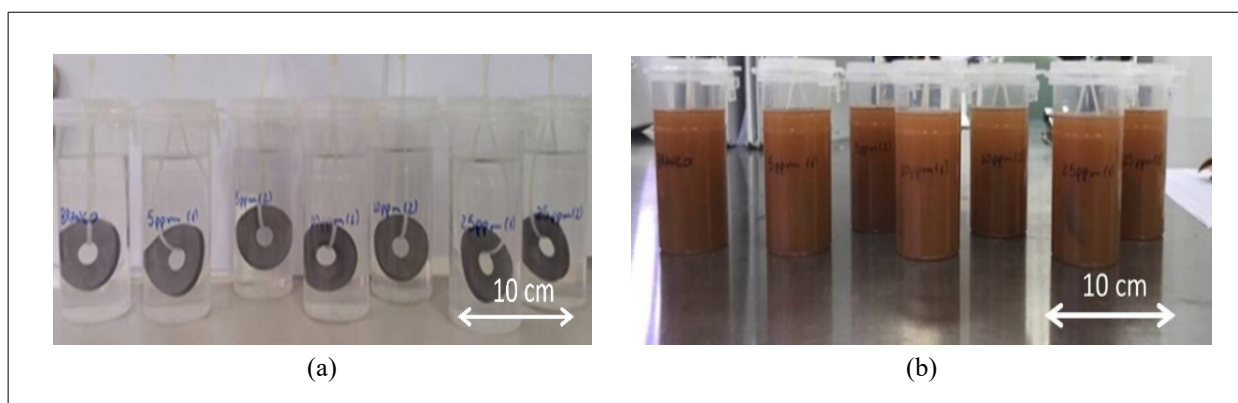
Note:  $\Phi$  = disc diameter,  $\Phi_{IM}$  = larger diameter,  $\Phi_{im}$  = smaller diameter  
(1) First sample; (2) Second sample

The coupons were subjected to the same test conditions used in the EIS analyses for a period of eight weeks (1,344 hours of exposure) in immersion cells, as shown



**Figure 2 ▼**  
Immersion cells used in the tests to determine mass loss. a) Beginning of the experiments. b) 1,344 hours of immersion.  
Source: authors' archive

in Figure 2. At intervals of eight days (192 hours), they were removed and subjected to chemical pickling in Clarke's solution, at room temperature, until the complete removal of oxidation products and residues adhered. They were then dried and weighed. Mass variations obtained in each weighing at the respective time intervals represent the corrosion rate.



The average corrosion rates ( $CR$ ) in  $\text{mm year}^{-1}$  and the inhibition efficiencies ( $Ef$ ) were determined using Equations 4 and 5, respectively (Abdallah *et al.*, 2018; Khaksar; Shirokoff, 2017). The qualitative classification of the corrosion rate is shown in Table 2.

$$CR = \frac{W \times 3.65 \cdot 10^5}{A \times T \times D} \quad (4)$$

where  $W$  is the mass loss (g);  $A$  is the initial exposed area ( $\text{mm}^2$ );  $T$  is the exposure time (days), and  $D$  is the metal density ( $\text{g/cm}^3$ ).

$$Ef = \frac{CR_S - CR_C}{CR_S} \times 100\% \quad (5)$$

where  $CR_S$  is the corrosion rate without an inhibitor ( $\text{mm/year}$ ) and  $CR_C$  is the corrosion rate with an inhibitor ( $\text{mm/year}$ ).

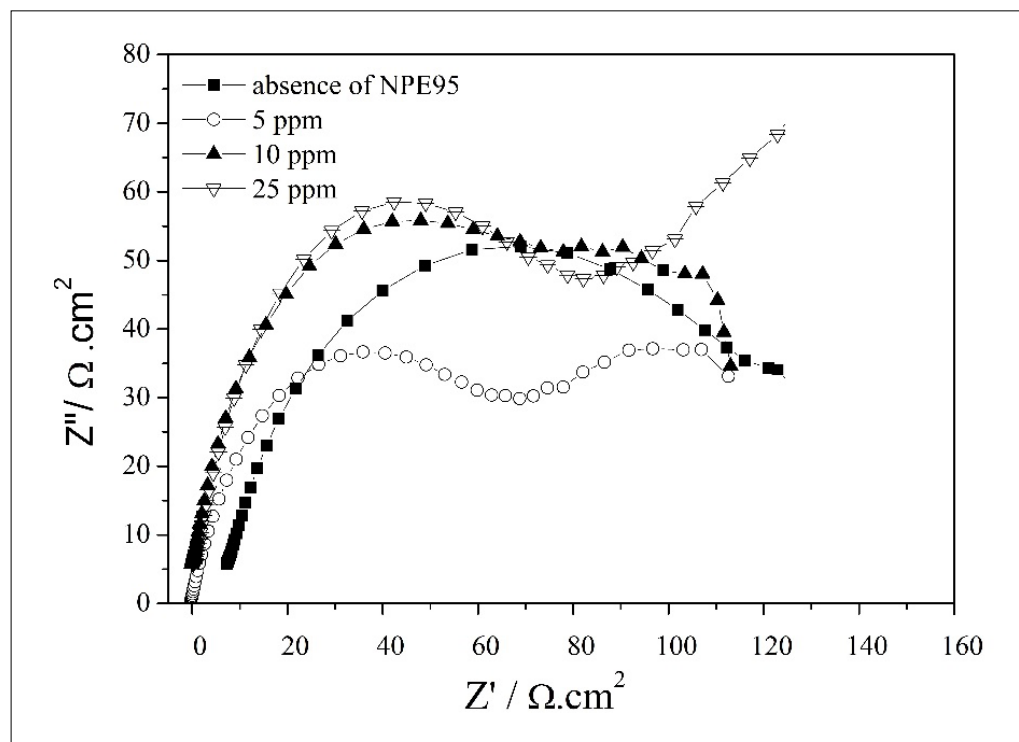
**Table 2 ►**  
Qualitative rating of uniform corrosion rate on coupons.  
Source: NACE International (1999)

Corrosion rate	(mm/year)
Low	< 0.025
Moderate	0.025 – 0.12
High	0.13 – 0.25
Severe	> 0.25

## 4 Results and discussion

Figure 3 presents the Nyquist diagrams obtained from the EIS analysis, which were used to evaluate the corrosion inhibition of SAE1020 steel by NPE95 at various surfactant concentrations.

**Figure 3** ▶  
Electrochemical impedance diagrams of SAE1020 steel in 3.0% NaCl medium, with and without the addition of NPE95.  
Source: research data



The diagram generated in the absence of the surfactant exhibits a single capacitive arc, indicative of a single charge transfer process, with total impedance associated with the corrosion resistance of the steel in the saline solution. There is no evidence of passivation film formation. In contrast, diagrams obtained with the addition of the surfactant display two capacitive arcs, suggesting enhanced corrosion inhibition. The first capacitive arc is attributed to the adsorbed film on carbon steel, while the second arc at low frequencies indicates a charge transfer process at the metal/electrolyte interface, or the corrosion process itself. An increase in the total resistance of the first capacitive arc is observed with increasing surfactant concentration, likely due to the adsorption of the surfactant on the surface of the working electrode, which increases with its concentration in the medium (Abdallah *et al.*, 2018; Fouda *et al.*, 2019).

Table 3 summarizes the polarization resistance ( $R_p$ ) obtained from electrochemical circle fitting and the adsorption efficiency ( $\theta$ ). Increasing the concentration of NPE95 effectively promoted greater inhibition of the corrosive processes, characterized by an increase in the total impedance modulus. This behavior has been observed and highlighted in related studies, such as those by Torres *et al.* (2016), where a correlation was noted between inhibitor concentration in the electrolytic medium and the corrosion rate of SAE1020 carbon steel under similar conditions to those in the present study.



**Table 3** ▶

Polarization resistance ( $R_p$ ) and adsorption efficiencies ( $\theta \times 100\%$ ) at various surfactant concentrations.

Source: research data

Surfactant concentration (ppm)	$R_p$ ( $\Omega$ )	Adsorbed molecules efficiency ( $\theta$ ) (%)
0	129.75	0.00
5	132.18	13.76
10	165.68	22.79
25	166.34	25.64

Adsorption curves derived from experimental  $R_p$  data and the fractions of molecules adsorbed on the surface ( $\theta$ ) are shown in Figures 4 and 5. These curves were compared with adsorption isotherm models from the literature, including Langmuir, Temkin, Flory-Huggins, and El-Awady (Foo; Hameed, 2010).

**Figure 4** ▶

Langmuir adsorption curve.

Source: research data

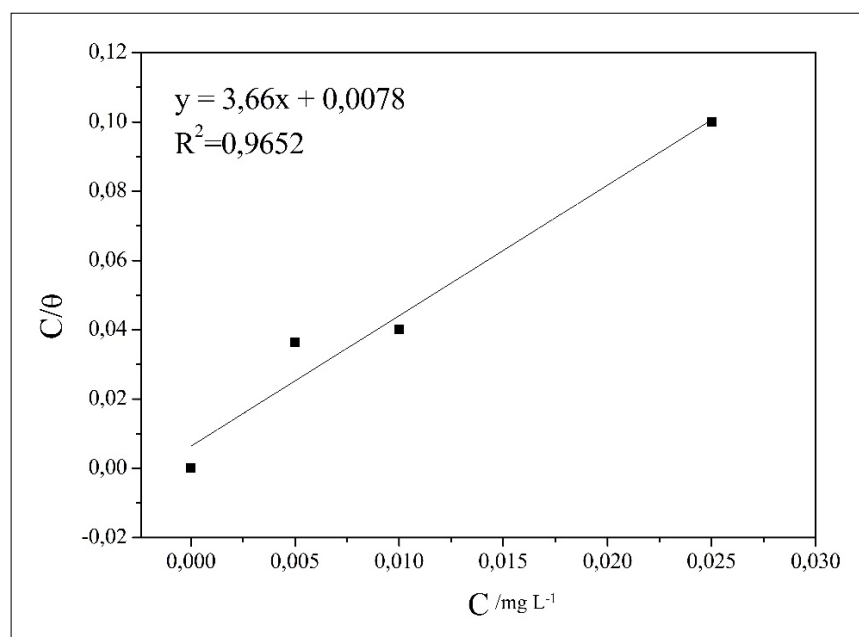
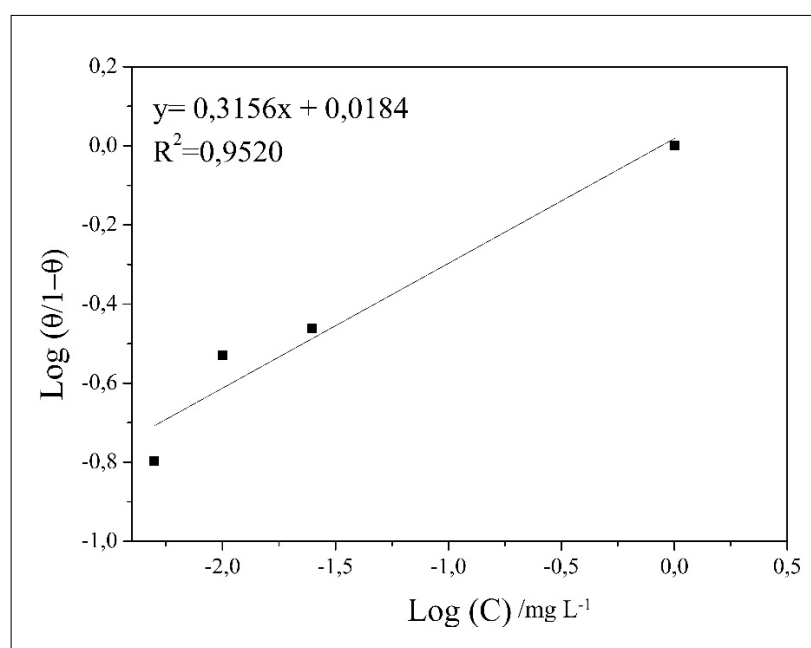


**Figure 5** ▶

El-Awady adsorption curve.

Source: research data



The Langmuir and El-Awady models, represented by Equations 6 and 7 respectively, provided the correlation coefficients ( $R^2 = 0.9652$  and  $R^2 = 0.9520$ ), consistent with good model fits as demonstrated by Boulinguez, Cloirec, and Wolbert (2008).

$$\frac{C}{\theta} = \frac{1}{K_{ads}} + C \quad (6)$$

$$\log \left[ \frac{\theta}{(1-\theta)} \right] = \log K_{ads} + y \log C \quad (7)$$

where  $C$  is the inhibitor concentration in  $\text{mg.L}^{-1}$ ;  $K_{ads}$  is the adsorption constant;  $\theta$  is the fraction of molecules adsorbed on the surface; and  $y$  is the number of inhibitor molecules adsorbed at an active site. From Equation 3, the  $\Delta G_{ads}$  values obtained using the Langmuir and El-Awady models were  $-21.987 \text{ kJ.mol}^{-1}$  and  $-10.061 \text{ kJ.mol}^{-1}$ , respectively, indicating spontaneous adsorption processes in the studied medium. According to Javadian, Yousefi, and Neshati (2013),  $\Delta G_{ads}$  values less negative than  $-20 \text{ kJ.mol}^{-1}$  are associated with physisorption.

**Table 4 ▼**

Relative mass losses and inhibition efficiencies of the NPE95 in 3% NaCl medium at various concentrations.

Source: research data

Data on total mass loss and inhibition efficiencies after exposure to the corrosive medium are shown in Table 4. The presence of NPE95 reduced the corrosion rate of steel in saline environments by approximately 17%. However, increasing the concentration of NPE95 from 5 ppm to 25 ppm did not significantly increase the inhibitor's efficiency. Thus, it can be inferred that the surfactant used in the study inhibited the corrosion process effectively.

NFP95 concentration (ppm)	Relative mass loss (%)	Inhibition efficiencies ( $E_f$ ) (%)
0	0.9702	-
5	0.8571	11.00
10	0.8312	13.58
25	0.8069	16.65

Figure 6 illustrates the relative mass losses of the coupons over time in the corrosive medium. As expected, and consistent with the EIS results, there is a tendency towards greater mass losses in the absence of the surfactant, with reductions as its concentration increases. However, the relative mass losses become subtle regardless of the presence and concentration of NPE95, indicating a reduction only in the kinetics of the processes without significant changes in the corrosion mechanisms (Torres *et al.*, 2016; Zhu; Free, 2016).

**Figure 6** ▶

Relative mass losses of coupons over time in 3.0% NaCl medium in the presence of the NPE95 at various concentrations.

Source: research data

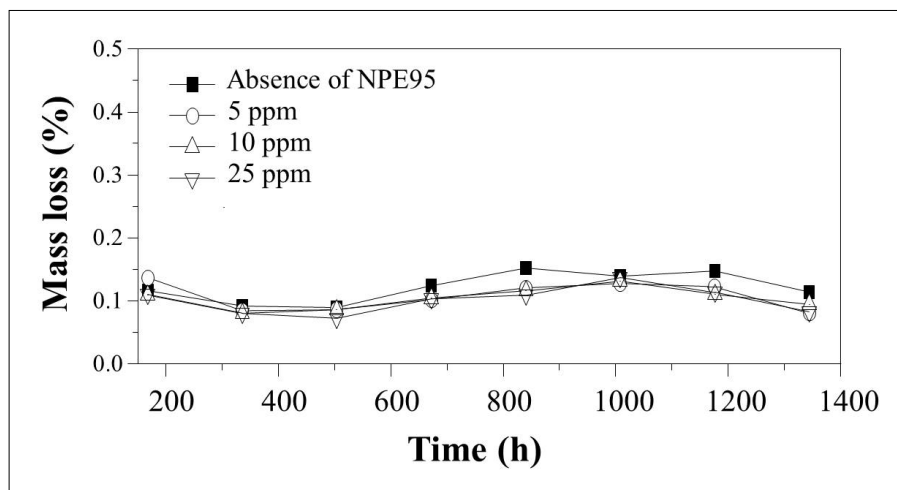
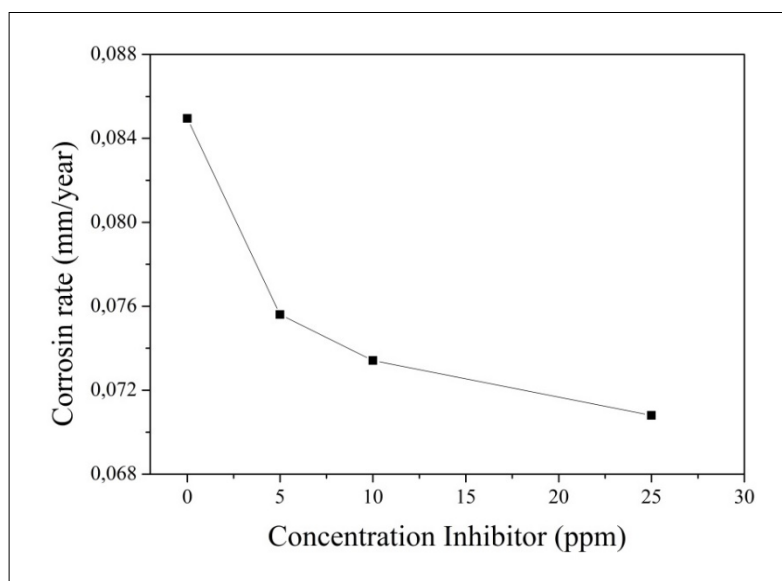


Figure 7 shows the influence of inhibitor concentration on the average corrosion rate over the 1,344-hour interval. Values were determined considering the specific mass of SAE1020 steel ( $7.85 \text{ g.cm}^{-3}$ ), mass losses of each electrode, and the respective exposed areas. The curve demonstrates that the corrosion rate decreases as the surfactant concentration increases, consistent with previous results. Corrosion rates in all specimens were considered moderate, according to NACE RP0775 (NACE International, 1999).

**Figure 7** ▶

Corrosion rate of the coupons over 1,344 hours of exposure in 3.0% NaCl medium.

Source: research data



## 5 Conclusion

The experimental results demonstrated that the surfactant nonylphenol polyethoxylated with a degree of ethoxylation of 9.5 (NPE95) effectively inhibited corrosion on SAE1020 steel in the studied medium. Both techniques employed in this study verified these findings.

Impedance results revealed that the presence of the inhibitor in the corrosive medium generated two capacitive arcs. The first capacitive arc is attributed to the adsorbed film on carbon steel, while the second, at low frequencies, indicates a charge transfer process at the metal/electrolyte interface, corresponding to the corrosion process. Increasing the

concentration of NPE95 effectively enhanced the inhibition of the corrosive processes, as evidenced by the increase in the total impedance modulus.

Data on total mass loss demonstrate that the presence of NPE95 resulted in an approximately 17% decrease in the corrosion rate of steel in saline environments.

These findings suggest that NPE95 demonstrates significant potential as a corrosion inhibitor for steels in saline mediums. However, further research involving higher concentrations of NPE95 or its combination with other additives may provide even more effective corrosion inhibition.

## Financial support

No significant financial support was received for this work that could have influenced its outcome.

## Conflicts of interest

No conflicts of interest are disclosed.

## Contributions to the article

**SILVA, G. P.:** conception or design of the study/research; data analysis and/or interpretation; final review with critical and intellectual participation in the manuscript. **SILVA FILHO, L. F.; ARAUO, A. A. L.; LIMA, R. N.:** final review with critical and intellectual participation in the manuscript **COSTA, V. A. F.; CARVALHO, S. C. F.:** conception or design of the study/research; data analysis and/or interpretation. All authors contributed to the writing, discussion, reading, and approval of the final version of the article.

## References

ABDALLAH, M.; HEGAZY, M. A.; ALFAKEER, M.; AHMED, H. Adsorption and inhibition performance of the novel cationic Gemini surfactant as a safe corrosion inhibitor for carbon steel in hydrochloric acid. **Green Chemistry Letters and Reviews**, v. 11, n. 4, p. 457-468, 2018. DOI: <https://doi.org/10.1080/17518253.2018.1526331>.

ARELLANES-LOZADA, P.; OLIVARES-XOMETL, O.; LIKHANOVA, N. V.; LIJANOVA, I. V.; VARGAS-GARCÍA, J. R.; HERNÁNDEZ-RAMÍREZ, R. E. Adsorption and performance of ammonium-based ionic liquids as corrosion inhibitors of steel. **Journal of Molecular Liquids**, v. 265, p. 151-163, 2018. DOI: <https://doi.org/10.1016/j.molliq.2018.04.153>.

ASTM INTERNATIONAL – AMERICAN SOCIETY FOR TESTING AND MATERIALS. **ASTM G1-03(2017)e1**. Standard practice for preparing, cleaning, and evaluation corrosion test specimens. West Conshohocken: ASTM, 1999. DOI: <https://doi.org/10.1520/G0001-03R17E01>.

BAJARES, R. A.; MELLA, L. Study of the corrosion rate in the couple of steels ASTM A-36 and AISI/SAE 304 in a water-coke of petroleum system. **Procedia Materials Science**, v. 8, p. 702-711, 2015. DOI: <http://dx.doi.org/10.1016/j.mspro.2015.04.127>.

BOULINGUIEZ, B.; CLOIREC, P.; WOLBERT, D. Revisiting the determination of Langmuir parameters-application to tetrahydrothiophene adsorption onto activated carbon. **Langmuir**, v. 24, n. 13, p. 6420-6424, 2008. DOI: <https://doi.org/10.1021/la800725s>.

BRYCKI, B. E.; KOWALCZYK, I. H.; SZULC, A.; KACZEREWKA, O.; PAKIET, M.; Organic corrosion inhibitors. In: ALIOFKHAZRAEI, M. (ed.). **Corrosion inhibitors, principles and recent applications**. [S.l.]: IntechOpen, 2017. p. 3-34. Available at: <https://www.intechopen.com/chapters/58695>. Accessed on: 9 Out. 2023.

DWIVEDI, D.; LEPKOVÁ, K.; BECKER, T. Carbon steel corrosion: a review of key surface properties and characterization methods. **RSC Advances**, v. 8, p. 4580-4610, 2017. DOI: <https://doi.org/10.1039/C6RA25094G>.

EL-HADDAD, M. A M.; RADWAN, A. B.; SLIEM, M. H.; HASSAN, W. M. I.; ABDULLAH, A. M. Highly efficient eco-friendly corrosion inhibitor for mild steel in 5 M HCl at elevated temperatures: experimental & molecular dynamics study. **Scientific Reports**, v. 9, 3695, 2019. DOI: <http://dx.doi.org/10.1038/s41598-019-40149-w>.

FARSAK, M.; KELES, H.; KELES, M. A new corrosion inhibitor for protection of low carbon steel in HCl solution. **Corrosion Science**, v. 98, p. 223-232, 2015. DOI: <https://doi.org/10.1016/j.corsci.2015.05.036>.

FOO, K Y; HAMEED, B H. Insights into the modeling of adsorption isotherm systems. **Chemical Engineering Journal**, v. 156, n. 1, p. 2-10, 2010. DOI: <https://doi.org/10.1016/j.cej.2009.09.013>.

FOUDA, A. S.; EL-ASKALANY, A.; EL-HABAB, A. T.; AHMED, S. Anticorrosion properties of some nonionic surfactants on carbon steel in 1 M HCl environment. **Journal of Bio- and Tribo-Corrosion**, v. 5, 56, 2019. DOI: <https://doi.org/10.1007/s40735-019-0248-2>.

GOYAL, A.; POUYA, H. S.; GANJIAN, E.; CLAISSE, P. A review of corrosion and protection of steel in concrete. **Arabian Journal for Science and Engineering**, v. 43, p. 5035-5055, 2018. DOI: <https://doi.org/10.1007/s13369-018-3303-2>.

JAVADIAN, S.; YOUSEFI, A.; NESHATI, J. Synergistic effect of mixed cationic and anionic surfactants on the corrosion inhibitor behavior of mild steel in 3.5% NaCl. **Applied Surface Science**, v. 285, Part B, p. 674-681, 2013. DOI: <http://dx.doi.org/10.1016/j.apsusc.2013.08.109>.

KHAKSAR, L.; SHIROKOFF, J. Effect of elemental sulfur and sulfide on the corrosion behavior of Cr-Mo low alloy steel for tubing and tubular components in oil and gas industry. **Materials**, v. 10, n. 4, 430, 2017. DOI: <https://doi.org/10.3390/ma10040430>.

MELO, R. P. F.; BARROS NETO, E. L.; MOURA, M. C. P. A.; DANTAS, T. N. C.; DANTAS NETO, A. A.; OLIVEIRA, H. N. M. Removal of reactive blue 19 using nonionic surfactant in cloud point extraction. **Separation and Purification Technology**, v. 138, p. 71-76, 2014. DOI: <https://doi.org/10.1016/j.seppur.2014.10.009>.

NACE INTERNATIONAL – NATIONAL ASSOCIATION OF CORROSION ENGINEERS. **NACE Standard RP0775-2005**. Standard Recommended Practice: Preparation, installation, analysis, and interpretation of corrosion coupons in oilfield operations. Houston: NACE International, 1999. Available at: <https://lopei.wordpress.com/wp-content/uploads/2011/07/nace-rp077505-evaluacion-de-cupones-de-corrosion-en-la-industria-petrolera.pdf>. Accessed on: 9 Out. 2023.

PEDEFERRI, P. Cathodic and anodic protection. *In*: LAZZARI, L.; PEDEFERRI, M. P. (ed.). **Corrosion Science and Engineering**. Cham: Springer, 2018. p. 383-422. DOI: [https://doi.org/10.1007/978-3-319-97625-9\\_19](https://doi.org/10.1007/978-3-319-97625-9_19).

REFAIT, P.; GROLLEAU, A.-M.; JEANNIN, M.; RÉMAZEILLES, C.; SABOT, R. Corrosion of carbon steel in marine environments: role of the corrosion product layer. **Corrosion and Materials Degradation**, v. 1, n. 1, p. 198-218, 2020. DOI: <https://doi.org/10.3390/cmd1010010>.

RIBEIRO, D. V.; SOUZA, C. A. C.; ABRANTES, J. C. C. Use of Electrochemical Impedance Spectroscopy (EIS) to monitoring the corrosion of reinforced concrete. **Revista IBRACON de Estruturas e Materiais**, v. 8, n. 4, p. 529-546, 2015. DOI: <https://doi.org/10.1590/S1983-41952015000400007>.

RODRIGUES, M. A. F.; ARRUDA, G. M.; SILVA, D. C.; COSTA, F. M. F.; BRITO, M. F. P.; ANTONINO, A. C. D.; WANDERLEY NETO, A. O. Application of nonionic surfactant nonylphenol to control acid stimulation in carbonate matrix. **Journal of Petroleum Science and Engineering**, v. 203, 108654, 2021. DOI: <https://doi.org/10.1016/j.petrol.2021.108654>.

SARKAR, R.; PAL, A.; RAKSHIT, A.; SAHA, B. Properties and applications of amphoteric surfactant: a concise review. **Journal of Surfactants and Detergents**, v. 24, n. 5, p. 709-730, 2021. DOI: <https://doi.org/10.1002/jsde.12542>.

SHABAN, S. M.; KANG, J.; KIM, D.-H. Surfactants: recent advances and their applications. **Composites Communications**, v. 22, 100537, 2020. DOI: <https://doi.org/10.1016/j.coco.2020.100537>.

TIWARI, S.; MALL, C.; SOLANKI, P. P. Surfactant and its applications: a review. **International Journal of Engineering Research and Application**, v. 8, n. 9, p. 61-66, 2018. Available at: <https://www.ijera.com/papers/vol8no9/p1/M0809016166.pdf>. Accessed on: 25 Mar. 2022.

TORRES, V. V.; CABRAL, G. B.; SILVA, A. C. G.; FERREIRA, K. C. R.; D'ELIA, E. Ação inibidora de extratos da semente do mamão papaia na corrosão do aço-carbono 1020 em HCl 1 mol.L<sup>-1</sup>. **Química Nova**, v. 39, n. 4, p. 423-430, 2016. DOI: <https://doi.org/10.5935/0100-4042.20160046>.

ZHU, Y.; FREE, M. L. Experimental investigation and modeling of the performance of pure and mixed surfactant inhibitors: micellization and corrosion inhibition. **Colloids and Surfaces A: Physicochemical and Engineering Aspects**, v. 489, p. 407-422, 2016. DOI: <http://dx.doi.org/10.1016/j.colsurfa.2015.11.005>.